Science of Sintering, **56** (2024) 445-453

https://doi.org/10.2298/SOS231031061P

UDK: 53.086; 519.718

Fractal Analysis and Microstructure Development PVDF Based Multifunctional Material

Adriana Peleš Tadić[1*)], George Vuković[2], Aleksandar Kojović[3], Dušica Stojanović[3], Branislav Vlahović[4], Nina Obradović[1], Vladimir B. Pavlović[5]

[1]Institute of Technical Sciences of SASA, Knez Mihailova 35/IV 11000 Belgrade, Serbia

[2]University of Wisconsin-Madison, USA

[3]Faculty of Technology and Metallurgy, University of Belgrade, Karnegijeva 4, 11120 Belgrade, Serbia

[4]North Carolina Central University, Durham, USA

[5]Faculty of Agriculture, University of Belgrade, Nemanjina 6, 11080 Belgrade, Serbia

Abstract:

Polyvinylidene fluoride (PVDF) is a novel gel polymer electrolyte alternative which can reduce the risk of irreversible failure in lithium-ion batteries (LIB) [1]. PVDF matrix structures which exhibit inter-crosslinking networks have previously demonstrated favorable thermal and mechanical properties for LIB applications [2]. PVDF based multifunctional material is attracting a great scientific interest due to its excellent piezoelectric, pyroelectric and ferroelectric properties. Such as, its properties strongly depend on synthesis procedures and obtained microstructures. In this research, porous structure and cross-linking patterns of PVDF were prepared by electrospinning method and it has been found that these microstructures can have fractal structure. Fractal analysis can be used as a powerful tool for describing structural and functional properties of these this material. Because of that, in this research we have used different fractal methods for the reconstructions of various PVDF microstructure morphologies. Fractal analysis has been performed by using scanning electron microscope micrographs and computational modeling tools. Theory of Iterated Function Systems and Voronoi tessellation, have been used for modeling PVDF porous structures. A Python algorithm was created to determine the distribution of pore areas in SEM micrographs. Algorithm's distribution of calculated pore surface areas were compared with measured pore surface areas and fractal reconstructions of different morphologies and their connection with functional properties were analyzed.

Keywords*: PVDF; Electrospinning; SEM; Fractal analysis; Voronoi tessellation.*

1. Introduction

Polyvinylidene fluoride (PVDF) represents a semicrystalline polymer with very good piezoelectric and pyroelectric properties [3, 4]. PVDF crystallizes in five different phases: alpha (α) phase, beta (β) phase, gamma (γ), etc. [5]. Beta and gamma phases, due to their crystal structure, have the best ferroelectric properties. PVDF normally exhibits α, the nonpolar phase, which is kinetically very stable. Due to that tendency, obtaining the electroactive β phase is difficult, so it is a big challenge to induce it in PVDF. For improving

*) **Corresponding author:** adriana.peles@itn.sanu.ac.rs

electroactive phases in PVDF, several techniques are usually in use. One of the techniques is adding a ceramics particles inside the polymer matrix as a filler. The most popular techniques, to provide β phase inside the polymer matrix, are the mechanical stretching of α-phase films at temperatures 70–100 ºC, adding a filler, and different types of synthesis. One of them is the electrospinning technique [6-8].

Electrospinning is a technology for producing polymer fibers and polymer composites with porous structure from polymer solutions and melts. The obtained fibers and pores are with micrometer or nanometer scale diameters. The process of electrospinning involves a high-voltage source to charge a polymer solution. After the applied voltage polymer solution accelerated towards a grounded metal collector of the opposite polarity. The polymeric fiber travels by evaporating the solvent from it allowing, thus leading to the deposition of solid polymer fibers on the collector. The basic electrospiner consists of a syringe filled with a polymer solution, a high-voltage source, and a grounded conductive collector screen [9]. Between the syringe's tip and the collector there is electric and electrostatic forces are generated and under its influence a pendant of polymer is formed. A pendant droplet of the polymer solution at the end of the syringe is deformed into the conical shape also known as the Taylor cone. The charge density increases at the tip of the cone. When the electrostatic forces overcome the surface tension of the polymer solution, a jet is ejected from the tip of the syringe [10, 11]. It has been found that nano-fiber like materials have very complex and porous structure that can be observed as fractal structure. As such, the fractal analysis can be used for describing structural and functional properties of this type of material.

Fractals are known as geometric shapes that display similarity through the full range of scale. They look the same no matter how big or small they are. Fractal objects are part of nature and they found their application in science, from cosmology to molecules. There are many examples of fractals that we encounter in everyday life such as Romanesco broccoli, pine cones, ice, snowflake, neurons, lungs tissue... that bear a comparable resemblance to "ideal" or "mathematical" fractals such as the Cantor set, Gosper contour, Koch curve, Sierpinski triangle/square, etc. [12]. The concept of a fractal is proposed by Mandelbrot in 1975, which refers to the graph, phenomenon, or process with self-similarity [13]. Fractals have the characteristics of self-similarity, scale invariants and self-affines [14-16]. There are three different types of Self-similarity. The first is called accurate (mathematical) fractal and it may be exactly similar to the Sierpiński triangle [17]. The other two types are known as random fractal [18] and it is the approximate similarity of branch bifurcation [19] and statistical similarity [20]. Scale invariant is the property that the shape, irregularity, and complexity of an object will not change if it is enlarged or shrunk in any local area of the object. This object can have fractal features in a scale invariant range [21]. Self-affine represents a special case of self-similarity. It refers that the proportion of transformation from local to global in diverse directions is not necessarily the same [21]. The feature of fractal objects can be described by fractal dimension. Fractal dimension (Hausdorff dimension) DH_f is a real number, to the contrast of topological dimension DT, where is $DT = 0$ for isolated points, $DT = 1$ for curves, $DT = 2$ for surfaces, $DT = 3$ for solids, etc. Therefore, Hausdorff dimension is in a range: $0 < DH_f < 1$ and covers all objects that are more than a point but less than a curve. If DH_f is between 1 and 2, the object is something between curve and surface [22]. Analytic method and fractal nature application is a new procedure in materials micro-structural characterization in order to reconstruct a materials structure, grains and pores, and make an advance prognosis of designed micro-structural properties [22]. The surface morphologies of all kinds of porous materials are complex and irregular, but they have features of self-similarity and as such can be analyzed by fractal theory. Fractal analysis represents a new approach for deeper examination of microstructure and for the prognosis of materials properties [23].

In order to define the pores and boundaries between pores inside PVDF based polymer composites obtained by electrospinning method, we used fractal analysis and Voronei tessellation.

2. Materials and Experimental Procedures

PVDF (M_w ~ 530 000) pelets was purchased from Sigma Aldrich and used without further purification). 22% solution (w/v) was prepared by dissolving 2.2 g of polymer in 10 ml dimethylformamide (DMF) (Sigma Aldrich). A homogenous solution of polymer was stirred at 70 °C, with 150 rpm for 3 h. The different samples were made by electrospinning process. The electrospinning apparatus used for the experiments was Electrospinner CH-01 (Linari Engineering, Italy). The voltage applied in experiments varied from 15 kV to 28 kV with the high-voltage supply (SPELMANN PCM50P120, USA), and the flow rate varied from 1 to 1.2 ml/h using syringe pumps of the R100E type (Razel Scientific Instruments, USA). The distance of the needle tip from the collector varied from 10 cm to 15 cm. All samples were obtained at 22 °C and 50% air humidity.

Morphology of PVDF porous film was investigated by a scanning electron microscope (JSM-6390 LV JEOL, Japan).

3. Results and Discussion

Fractal-like PVDF structures indicate that the pores have a repeating behavior. Computational modeling tools were utilized to identify pore dimensions using SEM images. This type of modeling was based on Voronei tessellation, which represent a visualization procedure for partitioning planes depending on the distance of points from a special subset of planes. The set of points (generator) is predetermined and for each there is a corresponding one the region consisting of all points that are closer to that generator than to any other [24]. These areas are called Voronei cells, and visually they form a Voronei tessellation, a "mosaic" of geometric shapes in a plane in which there are no overlaps or gaps. For two sets A and B with distance metric d(a,b) where a ∈ A and b ∈ B, a Voronoi diagram or tessellation is a subdivision of A into subsets, each of which contains the objects in A that are closer, with respect to the distance metric, to one object in B than to any other object in B [25]. A Voronoi diagram is sometimes also known as a Dirichlet tessellation. The cells are called Dirichlet regions, Thiessen polytopes, or Voronoi polygons. Our model used a cross correlation that represents a type of digital image processing method which can be used as a metric for determining the similarity between two images, or in this case pores. If a portion of pixels are arranged in a certain order, correlation algorithms can be programmed to determine that same arrangement of pixels in a different location. This indicates there is a 1:1 correlation [26]. To account for differences in brightness, the normalized cross correlation function is used as seen in the equation below. Ultimately, the pixel size and distribution are what determines correlation. The locations where the correlation is strong can be associated to a kernel. A kernel is a template of a specific arrangement of pixels which can be used as the basis for computing normalized cross correlation (Eq.1).

$$N_{tf}[i,j] = \frac{\sum_m \sum_n f[m,n]t[m-i,n-j]}{\sqrt{\sum_m \sum_n f^2[m,n]}\sqrt{\sum_m \sum_n t^2[m-i,n-j]}} \quad (1)$$

Normalized cross correlation equation is an adjusted version of the correlation equation to account for energy differences in signals, or in this case: brightness of each pore (Eq. 1).

To distinguish the boundaries between pores, a partition of areas must be computed. Voronoi tessellation (partition) is a geometric model which delineates regions using a set of points in a plane. As seen in Fig. 1, line segments connecting two points (kernels) guarantee the line segment connecting two neighbor points is perpendicular to the shared border and is bisected by that edge [25]. This method can essentially predict pore boundaries using geometric modeling.

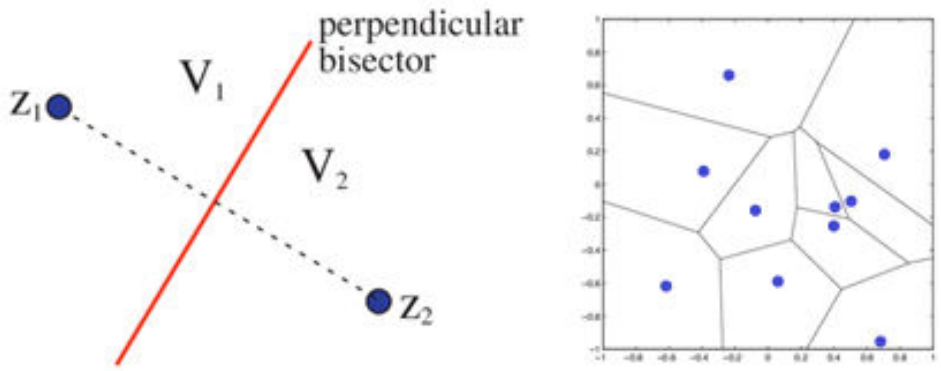

Fig. 1. Image A depicts the perpendicular bisector which separates Voronoi regions. Image B depicts a Voronoi partition in which the kernels are clearly shown to be separated by boundaries which are perpendicular bisectors to the inter-kernel line segment [27].

A Python algorithm (supported by SciPy, Scikit-image, and NumPy packages) was created to determine the distribution of pore areas in an SEM image. The algorithm requires a parameter image which can be thought of as the kernel. In this case, a singular pore (regardless of position or orientation) is chosen as the kernel. To determine local points of interest, a threshold parameter is set into the algorithm which limits the cross-correlation value, N_{tf} [i,j]. A higher N_{tf}[i,j] threshold indicates the local pores must be very similar to the kernel. While a low N_{tf} [i,j] threshold indicates a lower level of correlation. To map these values on an SEM image, a Sobel operator (filter) is applied, as shown in Fig. 2, which essentially filters the image to show a gradient of intensities. The algorithm translates the kernel across the image until it matches peaks that fall within the threshold parameter. These locations on the image get subsequently marked by a dot.

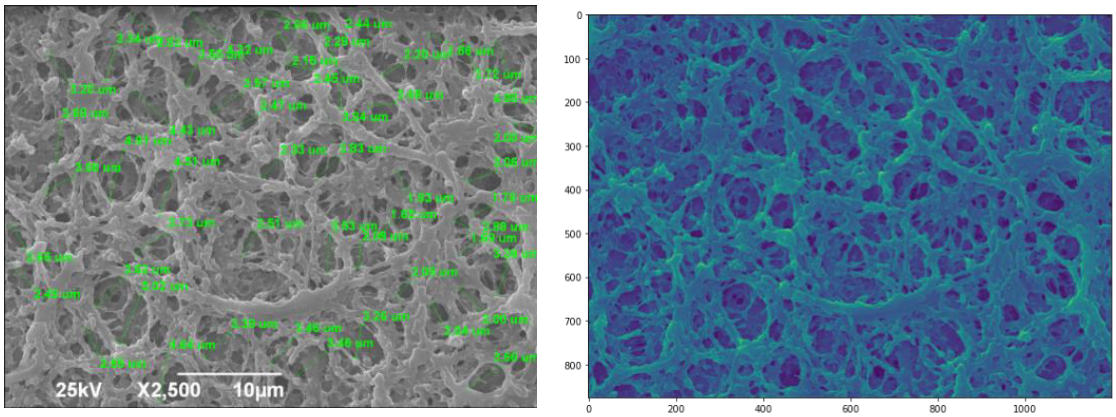

Fig. 2. Image A is of the PVDF fractal structure at 2.5K x magnification. The measurements shown in the image identify the diameter of the pore in question. Image B depicts the same image with the Sobel operator applied.

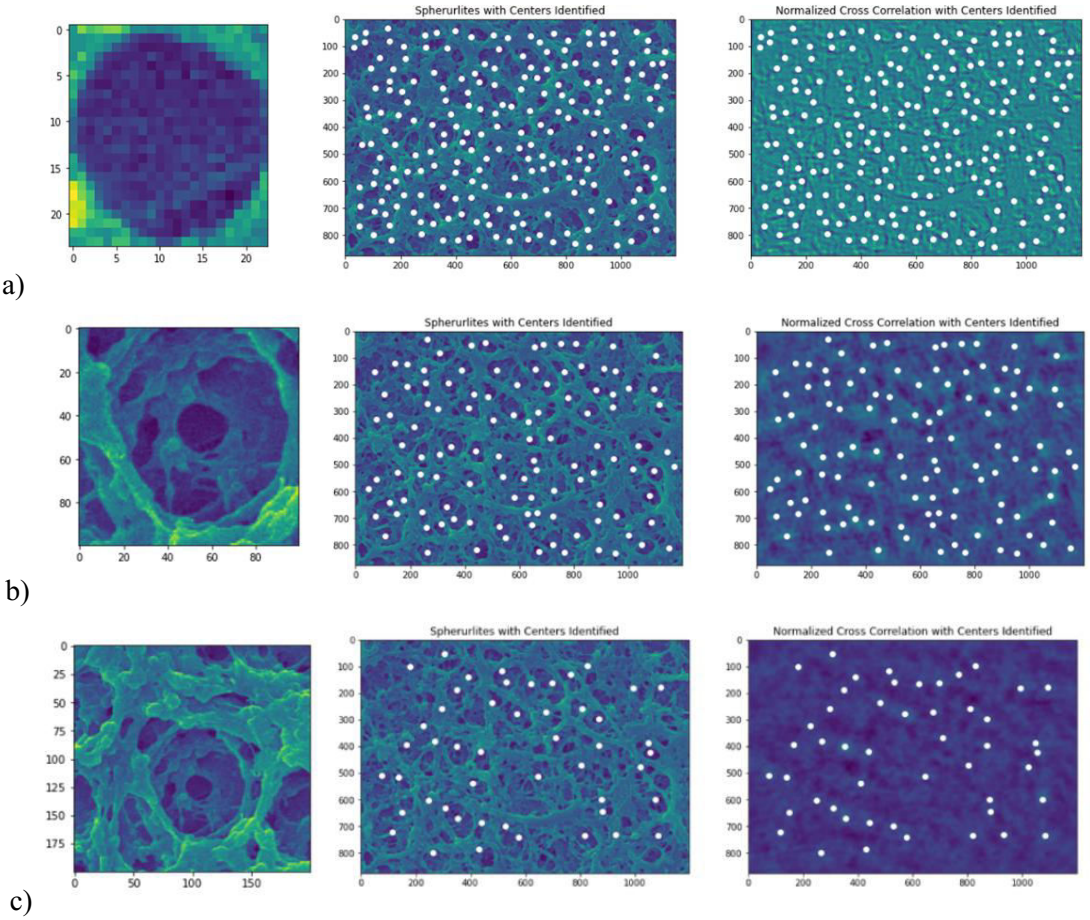

Fig. 3. The follow set of images represent the kernel size to output density relationship. A.) Kernel pixel dimensions = (414:438, 344:367), B.) Kernel pixel dimensions = (380:480, 300:400), C.) Kernel pixel dimensions = (300:500, 250:450). Threshold parameter = 0.09. These images were not filtered with the Sobel operator.

Fig. 3 depicts the cross-correlation accuracy depending on the kernel parameter chosen. Pores of the same dimensions as the kernel will be more accurately determined than ones that are not. In Fig. 3a, a smaller kernel, which predicts smaller pores, inconsistently determines larger pores. While for 3c, larger kernels accurately predict larger pores but are overshadowed by the exclusion of smaller pores. As seen in 3b, using a medium-sized kernel can detect a range of both large and small pores. By picking a medium-sized kernel, extreme pore sizes are not detected as the template parameter sacrifices extremes for consistency in detecting approximately average-sized pores.

The next portion of the algorithm utilizes Voronoi tessellation to delineate pore boundaries in relation to its nearest neighbors. Fig. 4 uses the kernel from Fig. 3b to generate the Voronoi partition with the addition of the Sobel filter. The algorithm accurately predicts pore boundaries that are near the center of the image. While the pores that are around the edges of the image get distorted as they do not have neighboring kernel points in all directions. As a result, certain pores are either overestimated or underestimated depending on its pixel configuration. This discretion is the major source of error in this algorithm which is represented in terms of the area distributions.

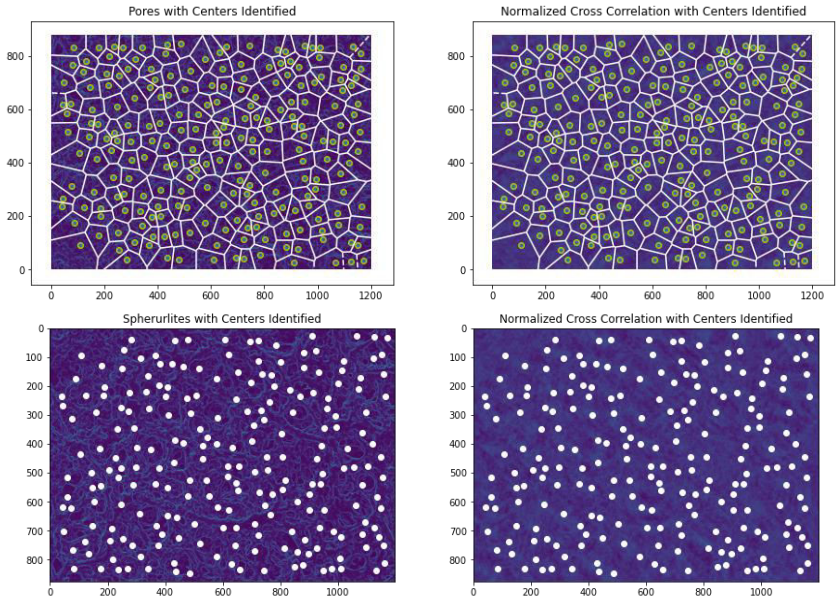

Fig. 4. The following diagrams show the normalized cross correlation with the Sobel operator applied onto the image. The green dots are indicative of the kernel matches while the white lines delineate the Voronoi partition.

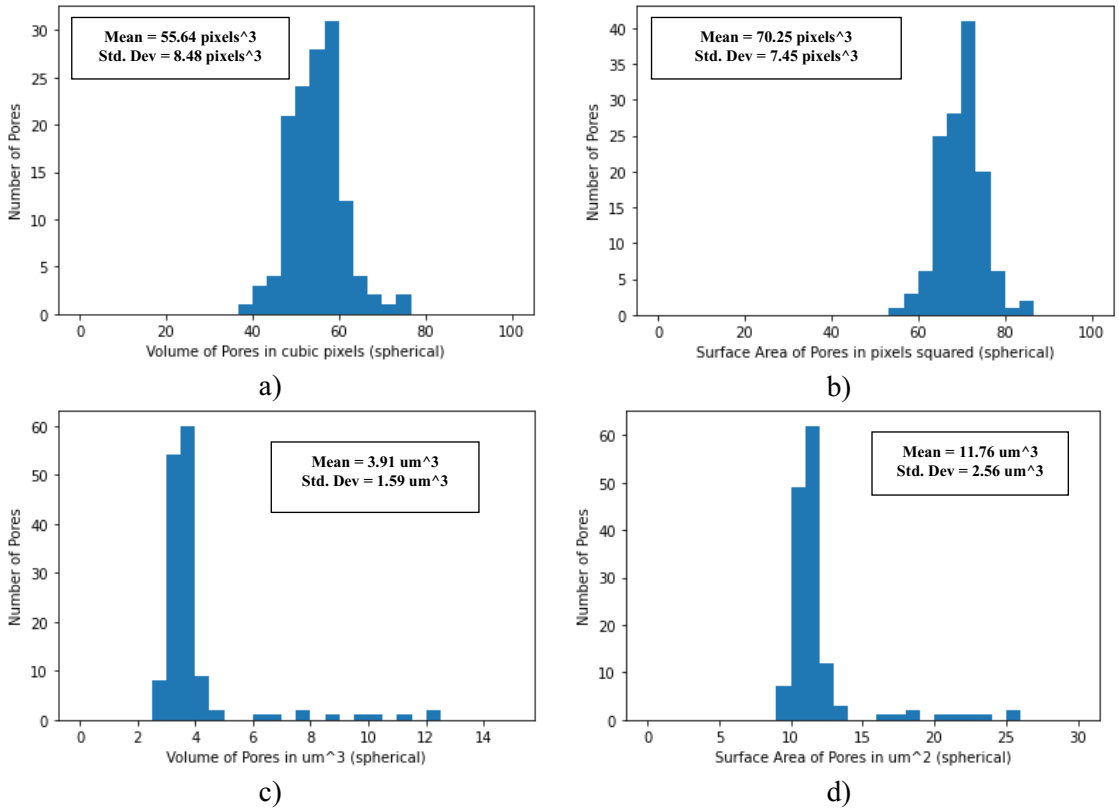

Fig. 5. Bar plots A and B represent the algorithm's distribution of calculated pore volumes and surface areas respectively Bar plot C and D represents the physically measured pore volume and surface areas. Using R-Studio the mean and standard deviations were calculated as seen in each plot.

The algorithm finally takes the Voronoi regions calculated and converts them into the pixelated area of each pore detected. Using the scale bar given in the Fig. 5, the pixel to μm ratio was found to be 250:10 (250 pixels = 10 μm). The distribution was then converted to μm where it was compared to physical SEM measurements of the same image in a bar plot. The physical measurements made a key assumption that all pores were approximated to have a surface area in the shape of a circle [$A=\pi(d/2)^2$]. Although most of the pores were not of circular shape, a generalized area needed to be assumed to accurately quantify the surface areas of each measured pore.

4. Conclusion

In this paper, we reported the investigation of the porous surface of the polymer composite, based on PVDF/ZnO polymer. The surfaces were obtained by SEM. Micrographs showed the fractal structure, so we used Voronoi tessellation to distinguish the boundaries between pores. This method can essentially predict pore boundaries using geometric modeling. A Python algorithm was created to determine the distribution of pore areas in an SEM image. At the end, the distribution was converted to μm and compared to physical SEM measurements of the same image. The physical measurements made a key assumption that all pores were approximated to have a surface area in the shape of a circle. Finally, both pore surface area and volume distributions seem to show similar arrangements. This indicates that the algorithm can predict similar distributions within a region. One trend that was readily apparent was the algorithm seemed to overestimate the size of the pores as the mean was higher and the skewness was more prominent. These indicators can be a result of the distortion of the pore boundaries the Voronoi tessellation could not account for at the edges of the image. One method of lessening the effects of boundary distortion could be to use images at lower magnification. Additionally, the algorithm also showed to have included regions which would be considered as strands of the PVDF. This unintentionally increased the average surface area of the pores. The physical calculations also made a major assumption in which all pores were subjected to being treated as a circular object. This distorted the actual surface areas as most of the pores did not confine to that shape. Further studies should be conducted on how an algorithm using Voronoi partition and normalized cross correlation can be adjusted and optimized to account for pores at image boundaries. A better method of physically measuring and determining pore sizes is also suggested as generalizing the shape is not a particularly accurate technique.

Acknowledgments

Funds for the realization of this work are provided by the Ministry of Science, Technological Development and Innovation of the Republic of Serbia, Agreement on realization and financing of scientific research work of the Institute of Technical Sciences of SASA in 2023 (Record number: 451-03-47/2023-01/200175), University of Belgrade, Faculty of Agriculture (Contract number: 451-03-47/2023-01/200116), University of Belgrade, Faculty of Technology and Metallurgy (Contract number: 451-03-68/2022-14/200135).

ORCID numbers:

Dr. Adriana Peleš Tadić, https://orcid.org/0000-0002-4970-5306
Prof. dr. Aleksandar Kojović, https://orcid.org/0000-0002-7608-9350
Prof. dr. Dusica Stojanović, https://orcid.org/0000-0001-6308-7586
Prof. dr. Branislav Vlahović, https://orcid.org/0000-0001-8965-1480
Prof. dr. Vladimir B. Pavlović, https://orcid.org/0000-0002-1138-0331

Dr. Nina Obradović, https://orcid.org/0000-0002-7993-293X

5. References

1. L.Porcarelli, A. S. Shaplov, F. Bella, J. R. Nair, D. Mecerreyes, C. Gerbaldi, Single-Ion Conducting Polymer Electrolytes for Lithium Metal Polymer Batteries that Operate at Ambient Temperature. ACS Energy Lett. 1 (2016) 678−682.
2. Q. Xiao, C. Deng, Q. Wang, Q. Zhang, Y. Yue, S. Ren, In Situ Cross-Linked Gel Polymer Electrolyte Membranes with Excellent Thermal Stability for Lithium-Ion Batteries. ACS Omega, 4 (2019) 95−103.
3. D. A. Seiler, Modern Fluoropolymers. Edited by John Scheirs © 1997 John Wiley & Sons Ltd, Wiley (1997) 487–505.
4. G.W. Taylor, J.J. Gagnepain, T.R. Meeker, T. Nakamura, L.A. Shuvalov, Piezoelectricity. New York: Gordon and Breach Science Publishers (1985).
5. Q.Xunlin, Patterned piezo-, pyro-, and ferroelectricity of poled polymer electrets, J. Appl. Phys., 108 (2010) 011101.
6. J.S. Humphrey, R. Amin-Sanayei, Vinylidene fluoride polymers, New York: Wiley; (2002) pp. 392.
7. T. Furukawa, Ferroelectric properties of vinylidene fluoride copolymers, Phase Transit. 18 (1989) 143–211.
8. A.J. Lovinger, Ferroelectric Polymers, Science 220 (1983) 1115–1121.
9. T.J. Sill, H. A. Von Recum, Electrospinning: Applications in drug delivery and tissue engineering, Biomaterials, 29, (2008) 1989−2006.
10. L.V. Schueren, B.D. Schoenmaker, O.I. Kalaoglu, K.D. Clerck, An alternative solvent system for the steady state electrospinning of polycaprolactone, European Polymer Journal, 47, (2011) 1256−1263.
11. K. Garg, G.L. Bowlin, Electrospinning Jets And Nanofibrous Structures, Biomicrofluids, 5, (2011) 013403.
12. V. Vučković, V.V. Mitić, Lj. Kocić, V. Nikolić, The Fractal Nature Approach in Ceramics Materials and Discrete Field Simulation, Science of Sintering, 50 (2018) 371−385.
13. B.B. Mandelbrot, Stochastic Models for the Earth's Relief, the Shape and the Fractal Dimension of the Coastlines, and the Number-area Rule for Islands. Proc. Natl. Acad. Sci. USA 72, (1975) 3825–3828.
14. F. Wen, H. Fan, S. Zhai, K. Zhang, F. Liu, Pore characteristics analysis and numerical seepage simulation of antifreeze permeable concrete. Constr. Build. Mater., 255, (2020), 119310.
15. A.E. Sand, S.L. Dudarev, K. Nordlund, High-energy collision cascades in tungsten: Dislocation loops structure and clustering scaling laws. EPL. 103 (2013) 46003.
16. N.A. Fataf, A. Gowrisankar, S. Banerjee, In search of self-similar chaotic attractors based on fractal function with variable scaling approximately. Phys. Scr., 9 5 (2020)075206.
17. Z. Jiang, D. Liu, M. Chen, J. Wang, H. Zhao, Y. Li, Z. Zhang, T. Xie, F. Wang , X. Li, G.R. Newkome, P. Wang, Assembling Shape-Persistent High-Order Sierpiński Triangular Fractals, iScience, 23 (2020) 101064.
18. T. Hasegawa, S. Mizutaka, Structure of percolating clusters in random clustered networks. Phys. Rev. E., 101 (2020) 101.
19. L. Dong, Mechanical response of Ti–6Al–4V hierarchical architected metamaterials. Acta Mater., 175 (2019) 90–106.
20. X. Ding, X. Xiao, X.-F. Lv, D. Wu, Y. Pan, Analysis of Similarities and Differences between Acoustic Emission and Charge Signal Based on Fractal Characteristics of Coal Fracture. Adv. Civ. Eng., (2020) 1–12.
21. Q. Duan, J. An, H. Mao, D. Liang, H. Li, S. Wang, C. Huang, Review about the

Application of Fractal Theory in the Research of Packaging Materials. Materials 14, (2021) 860.
22. V. Mitić, G.M. Lazović, J. Ž. Manojlović, W.-C. Huang, M.M. Stojiljković, H. Facht, B. Vlahović, Entropy and Fractal Nature, Thermal science, 24, 3 (2020) 2203−2212.
23. J. Purenović, V. V. Mitić, Lj. Kocić, V. Pavlović, M. Randjelović, M. Purenović, Intergranular Area Microalloyed Aluminium-silicate Ceramics Fractal Analysis, Science of Sintering, 45 (2013) 117−126
24. V. V. Mitić, V. Paunović, S. Janković, V. Pavlović, I. Antolović, D. Rančić, Electronic Ceramic Structure within the Voronoi Cells Model and Microstructure Fractals Contacts Surfaces New Frontier Applications,Science of Sintering, 45 (2013) 223−232.
25. L. Ju, T. Ringler, M. Gunzburger, Voronoi Tessellations and Their Application to Climate and Global Modeling, Numerical Techniques for Global Atmospheric Models, Ch. 10, (2011).
26. K. Briechle, U.D. Hanebeck, Template matching using fast normalized cross correlation. Proc. SPIE 4387, Optical Pattern Recognition XII, (20 March 2001)
27. J. Burkardt, M. Gunzburger, J. Peterson, R. Brannon, Rebecca, User Manual and Supporting Information for Library of Codes for Centroidal Voronoi Point Placement and Associated Zeroth, First, and Second Moment Determination, U.S. Department of Energy Office of Scientific and Technical Information, (2002).

Сажетак: *Поливинилиден флуорид (ПВДФ) је нова алтернатива гел полимеру електролита која може смањити ризик од неповратног квара у литијум-јонским батеријама (ЛИБ) [1]. ПВДФ матричне структуре које показују мреже међусобног умрежавања су раније показале повољна термичка и механичка својства за ЛИБ апликације [2]. Мултифункционални материјал на бази ПВДФ-а привлачи велико научно интересовање због својих одличних пиезоелектричних, пироелектричних и фероелектричних својстава. На пример, његове особине у великој мери зависе од поступака синтезе и добијених микроструктура. У овом истраживању, порозна структура и обрасци умрежавања ПВДФ-а су припремљени методом електроспиновања и утврђено је да ове микроструктуре могу имати фракталну структуру. Фрактална анализа се може користити као моћно средство за описивање структурних и функционалних особина ових материјала. Због тога смо у овом истраживању користили различите фракталне методе за реконструкцију различитих морфологија ПВДФ микроструктуре. Фрактална анализа је извршена коришћењем микрографија скенирајућег електронског микроскопа и алата за рачунарско моделирање. Теорија система итерираних функција и Воронојева теселација су коришћени за моделовање ПВДФ порозних структура. Направљен је Пајтон алгоритам за одређивање дистрибуције површина пора на СЕМ микрографијама. Алгоритамска дистрибуција израчунатих површина пора је упоређена са измереним површинама пора и анализиране су фракталне реконструкције различитих морфологија и њихова повезаност са функционалним својствима.*
Кључне речи*: ПВДФ, електроспиновање, СЕМ, фрактална анализа, Воронојева тесалација.*